WEATHERING OF CHLORITE TO A LOW-CHARGE EXPANDABLE MINERAL IN A SPODOSOL ON THE APENNINE MOUNTAINS, ITALY

STEFANO CARNICELLI,[1] ALDO MIRABELLA,[2] GUIA CECCHINI[1] AND GUIDO SANESI[1]

[1]Dipartimento di Scienza del Suolo e Nutrizione della Pianta, Università di Firenze, P.le Cascine 16, 50144 Firenze, Italy

[2]Istituto Sperimentale per lo Studio e la Difesa del Suolo. MiRAAF P.za D'Azeglio 30, 50121 Firenze, Italy

Abstract—The clay fraction of a Spodosol and its parent rock in the Apennine mountains of central Italy were studied by powder X-ray diffraction (XRD) and infrared (IR) spectroscopy, to evaluate the possibility of transformation of chlorite into low-charge expandable minerals. Results indicated that the main phyllosilicate in the rock was a slightly weathered trioctahedral chlorite, rich in both Mg and Fe, together with dioctahedral mica and minor amounts of kaolinite. In the BC horizon, chlorite has undergone partial transformation into 2 vermiculitic components, in 1 of which the interlayer could be removed by hot Na-citrate treatment; the presence of a regular interstratified mineral (high-charge corrensite) was also observed. Further changes in the structure of chlorite were detected in the Bs1 horizon, becoming more evident towards the soil surface. The first stage of weathering of chlorite involved Fe oxidation and partial expulsion of Mg from the hydroxide sheet, followed by deposition of Al in the interlayer space. Iron is also removed from the interlayer sheet, possibly remaining, in the oxidized state, in the 2:1 octahedral sheet, and so contributing to the lowering of layer charge and transformation to a dioctahedral structure. When approaching the surface, Al removal from the interlayers is enhanced by complexing agents, and further charge reduction leads to the formation of 2:1 minerals with a smectite nature. Illite, because of its low content in the soil clay fraction, contributes marginally to this weathering sequence, forming the high charged expandable component observed in the Bhs horizon. At the soil surface, a randomly interstratified vermiculite/illite was detected, which probably originated from K fixation by the higher-charged expandable minerals. This study of weathering in a natural soil strongly supports the hypothesis, previously ascertained by laboratory experiments, that chlorite can transform into a low-charge expandable mineral.

Key Words—Chlorite, Hydroxy-interlayers, Smectite, Spodosols.

INTRODUCTION

Since the reviews by Ross (1980) and Wilson (1986), the concept of a typical clay mineral sequence for podzolic soils has become well-established. Such a typical sequence is characterized by the presence of chlorite and/or chlorite-vermiculite intergrades, successively referred to as "HIV" or "HIM", in the deep illuviation horizons and by the disappearing of such minerals, with the appearance of either vermiculite or smectite in the E horizon. The smectites in Spodosols were reported by Ross (1980) as having some properties usually associated with vermiculites, this being due either to a relatively high layer charge and/or to concentration of the charge in the tetrahedral sheets.

Subsequent work on identification of smectite and vermiculite, reviewed by Douglas (1989), has outlined the problems in discriminating these 2 minerals by conventional EG or glycerol solvation procedures, so it is likely that earlier authors were in fact considering a continuum between low-charge vermiculites and high-charge smectites, the interpretation depending on the procedure used or on small differences in actual charge.

Ross (1980) discussed the commonly held view that chlorite absence from the E horizons of Spodosols was due to chlorite destruction, and pointed out how laboratory weathering experiments had demonstrated the possibility of dioctahedral smectites forming from chlorites through removal of hydroxy interlayers and reduction of layer charge. Successive experiments (Senkayi et al. 1981) have further evidenced this possibility.

Formation of smectite, or EG-expandable vermiculite, from hydroxy-interlayered minerals (HIM), these last originated by pedogenic intercalation of pre-existing expandable phyllosilicates, has been reported (Malcolm et al. 1969; April et al. 1986). April et al. (1986) also considered, as an alternative hypothesis, that the HIM minerals might never have formed in the surface horizons of the Spodosols they studied where the presence of organic acids would hamper Al deposition.

Recent work on both Spodosols and environmentally associated Dystrochrepts (Righi and Meunier 1991; Righi et al. 1993) has again reported the presence of smectite (identified by EG solvation) components in surface horizons, and of HIM in the B horizons. The authors have, in one case, traced possible origins to either chlorite or mica (Righi et al. 1993), while in the other case (Righi and Meunier 1991) they have attributed the genesis of the low-charge expandable mineral to weathering of mica, although chlorite was present in the parent material. This last interpretation was based again on the concept of chlorite de-

Table 1. Basic physico-chemical characters of the soil examined (profile 11).

Hori-zon	Limits cm	Moist color (Munsell)	Sand %	Silt %	Clay %	pH H_2O	C org. %	ECEC cmol$^+$ kg^{-1}	Fe$_d$†	Fe$_o$‡	Fe$_p$§	Al$_d$†	Al$_o$‡	Al$_p$§
											g kg^{-1}			
E	1/1.5–3	10YR 3/2	52.9	28.8	18.3	3.4	9.2	6.7	9.1	4.8	4.4	1.9	2.4	2.0
Bhs	1.5–3/7–8	5YR 3/2	48.7	30.9	20.4	3.9	3.8	7.5	15.7	10.5	8.2	3.7	4.4	3.8
Bs1	7–8/20–21	7.5YR 4/4	41.2	31.5	27.3	4.5	2.7	4.5	20.0	14.3	10.1	7.0	6.1	6.0
Bs2	20–21/27–28	7.5YR 4/4	44.4	37.6	18.0	4.6	1.5	2.6	10.9	9.5	5.0	6.6	7.1	6.0
BC	27–28/60	10YR 5/4	52.8	31.6	15.6	4.8	0.7	2.0	6.5	4.8	2.7	4.6	4.8	3.6

† d = extractable by DCB.
‡ o = extractable by acid NH_4-oxalate.
§ p = extractable by Na-pyrophosphate.

struction in acid environments. The possibility of transformation of chlorite to smectite has, however, been demonstrated not only by laboratory experiments, but also in a natural soil, developing in a different, but still severe, weathering environment (Herbillon and Makumbi 1975).

Kaolinite is not a very common component of Spodosol clay fraction; Ross (1980) pointed out how this is in apparent disagreement with thermodynamic equilibrium calculations, and endorsed the view that this contrast is due to incomplete evolution, and then non-equilibrium, of soils that, in most cases, are geologically young and develop in rather cool climates.

Recently, a different point of view on the nature and weathering of HIMs was presented (Wada et al. 1991; Cho and Mermut 1992). The interlayer materials of the minerals they studied was rich in Si and displayed some typical properties of kaolinite; Cho and Mermut (1992) found that the mineral evolved to a true 1:1 layer silicate that the authors termed "halloysite", on the basis of morphological evidence.

The study of the clay mineralogy of a Spodosol in the Apennine mountains of central Italy may provide further knowledge about the possibility of transformation of chlorite into low-charge expandable minerals in this soil type.

MATERIALS AND METHODS

The soil under study is located on the southern slope of Tuscan-Emilian Apennines, lat 44°07'N, long 10°40'E; elevation is about 1200 m MSL; climate is rather cold and humid, with average annual rainfall of 2552 mm and temperature of 6.7 °C. Summer temperatures are much higher, about 15.9 °C diurnal average, and a pronounced dry period spans July and August, with a monthly rainfall average of 73 mm.

In this area, soils develop from the Macigno formation, of Oligocene to Miocene age, a turbiditic sequence made up of thick sandstone layers intercalated by thin mudstone ones (Dallan et al. 1981). Specifically of interest to this study, soils develop on coarse drift, dominated by the sandstone component.

Four soil profiles were excavated in a European beech (*Fagus sylvatica*) stand, approximately 120 y

old; 2 profiles were located within 1 m of a tree trunk and 2 at 1 to 2 m distance. All soil profiles were located on a broad shoulder, with about 20% average slope; there are strong indications that the soils examined have been subjected to significant erosion, as indicated by uncovering of old plants' collars and by the thinness and partial development of upper horizons. All soils were classified as Typic Haplorthods, though placed at the border with Inceptisols because of limited development of the upper diagnostic horizons; it appears to us that this situation can be associated with truncation of the profile, and that upper diagnostic horizons are now reforming at the expense of the underlying ones. Routine mineralogical characterization indicated similarity of all profiles; therefore, in-depth investigations were carried out on 1 profile only, and are reported here. The main soil properties are reported in Table 1.

Fresh rock samples were ground in an interval-operating mill to avoid heating. Soil clay (<2 μm) was separated from the fine earth fraction by sedimentation, after dispersion in water with addition of calgon as a dispersing agent; samples from the surface horizons (E and Bhs) were pretreated with unbuffered hydrogen peroxide to remove organic matter. Specimens were then Mg-saturated, washed free of chlorides and freeze-dried.

The rock samples were subjected to boiling in 6 N HCl for 30 min, to dissolve trioctahedral chlorite (Wilson 1987). Removal of interlayer hydroxy polymers was carried out by a modification of the Tamura (1958) procedure, in which a contact time of 24 h without extractant renewal has been obtained by heating the samples in autoclave.

X-ray patterns of ground rock and soil clay (<2 μm) were obtained from samples oriented on glass slides on a 3-kW Rigaku D/MAX III C diffractometer, equipped with a horizontal goniometer, a curved-beam graphite monochromator and Cu radiation. Slides were step-scanned either from 2 to 15 or from 2 to 35 °2θ, with steps of 0.02 °2θ and counting time of 4 s. The following treatments were performed: ethylene glycol solvation and K-saturation, followed by heating for 2 h at 350 and 550 °C. Random powder mounts were
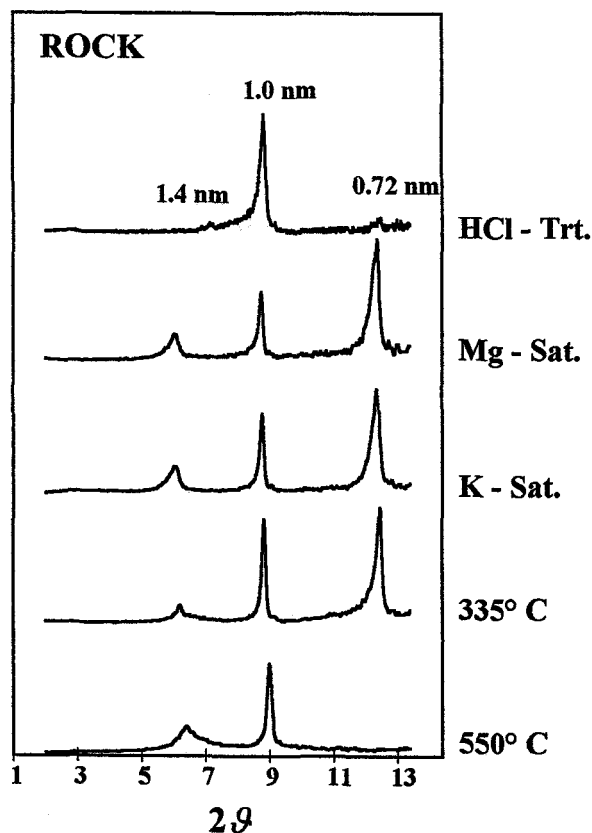
ROCK

Figure 1.   X-ray patterns of ground parent rock, smoothed and corrected for Lorentz and polarization factors. "HCl-Trt." refers to sample treated with boiling 1 *N* HCl: all other diagnostic treatments were carried out on untreated sample.

prepared by backfilling Al holders and gently pressing over filter paper, from soil clays and both untreated and HCl-treated rock samples. Random mounts were step-scanned at 0.02 °2θ increments with 30-s counting time for examining the $d(060)$ region of phyllosilicates and for more precise determination of peak positions, when necessary.

Digitized X-ray data were routinely smoothed and corrected for Lorentz and polarization factors (Moore and Reynolds 1989). Peak separation and profile analysis were carried out by an improved version of the program described by Enzo et al. (1988), which assumes single peaks to be described by a Pseudo-Voigt function (Howard and Preston 1989). Initial estimates of peak positions, intensities and widths at half-height are supplied to the software from visual examination of the X-ray pattern. The program reconstructs single peaks by fitting the envelope curve of overlapping peaks; the Marquardt algorithm is used in the improved version, instead of the simplex method used by Enzo et al. (1988). This procedure also outputs integral intensity (area) of each single peak.

IR spectra of ground rock and soil clay (<2 μm) were obtained on a Perkin-Elmer 880 spectrometer. Three kinds of spectra were recorded: 4000 to 400 cm^{-1} on pellets made with 1 mg of sample and 250 mg of KBr (full); 4000 to 3000 cm^{-1} on the same pellets heated at 150 °C to eliminate absorbed water (H); and 1400 to 400 cm^{-1} on pellets made with 0.3 mg of sample and 250 mg of KBr (HD). Differential spectra of the rock samples were obtained by subtracting spectra of HCl-treated samples from those of the untreated ones.

RESULTS

Characterization of Parent Rock Phyllosilicates

X-ray diffractograms of the Mg-saturated and oriented rock sample showed 3 peaks, at 1.44, 1.02 and 0.72 nm (Figure 1). The latter one could be split by profile fitting into 2 components at 0.719 and 0.711 nm. No modification was induced by K-saturation, while heating at 335 °C resulted in a slight decrease of the intensity ratio between the 1.44- and the 1.03-nm peaks. Upon heating at 550 °C, the 1.44-nm peak was reinforced, while the 0.7-nm components disappeared. Treatment by HCl, followed by Mg saturation, resulted in disappearance of the 1.44-nm peak, while a small one remained at 0.7 nm (Figure 1). This behavior indicates the presence of a slightly weathered chlorite. Weathering is evidenced by the reduced thermal stability of $d(001)$ at 335 °C and by strong dehydroxylation of the interlayer at 550 °C. The trioctahedral nature of the chlorite, inferred by easy dissolution in HCl, is confirmed by observation of a $d(060)$ peak at 0.153 nm that could be separated from the strong quartz interference, and which disappeared after HCl treatment.

Other phyllosilicate components of the parent rock are mica and a small amount of kaolinite, revealed by the small 0.7-nm peak in the HCl-treated sample. The mica component is dioctahedral, as revealed by a significant $d(002)$ peak at about 0.5 nm and by the position of the $d(060)$ peak at 0.151 nm This component probably has an illitic nature, as inferred by its low stability in the soil (*vide infra*).

An approximate structural formula for chlorite was estimated from positions and intensity ratios of the various basal reflections. Tetrahedral Al-for-Si substitution was obtained from the formula:

$$d(001) = 14.648 \text{ Å} - 0.378x \qquad [1]$$

where x = tetrahedral Al over 4 tetrahedral cations (Bailey 1975, Eq. 5).

Total Al was then obtained from:

$$d(001) = 14.52 \text{ Å} - 0.14x \qquad [2]$$

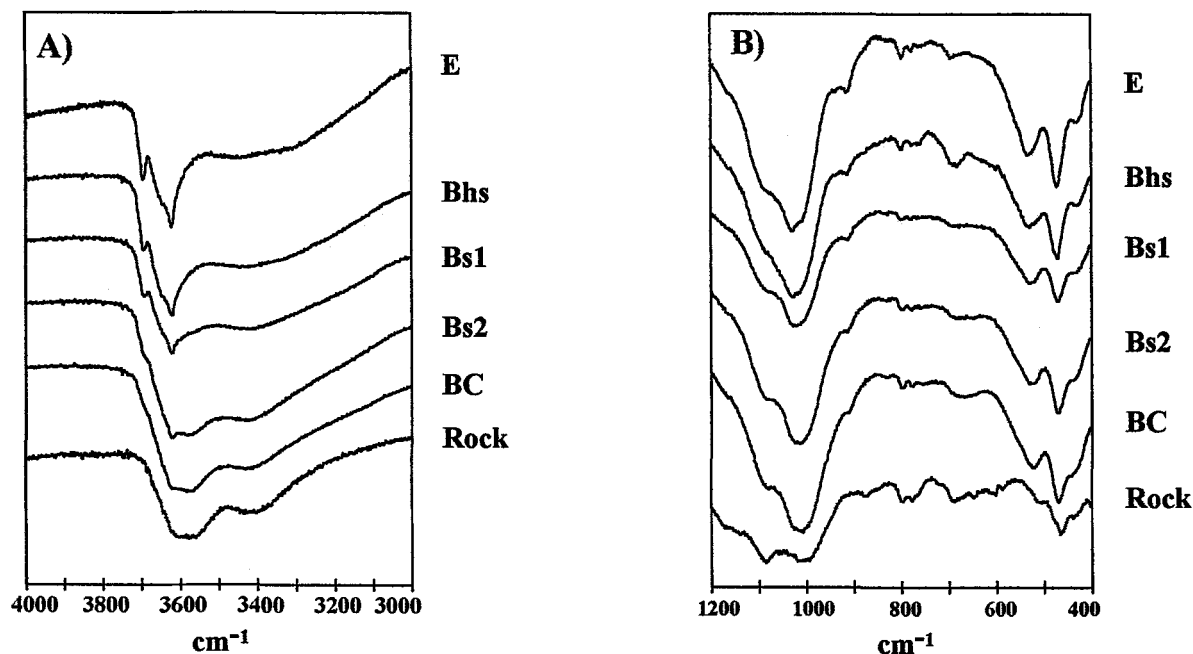where x = total Al and Cr over 10 total cations (Bailey 1975, Eq. 3); Cr has been considered negligible.

Figure 2.   IR spectra of soil clays (<2 μm) and differential IR spectra of HCl-soluble portion of parent rock. A) OH-stretching region, 1 mg 300 mg^{-1} KBr, heated at 150 °C for 16 h; B) OH-bending and M-O region, 0.3 mg 300 mg^{-1} KBr.

Total Fe and Fe distribution were estimated as reviewed by Brown and Brindley (1980); the degree of asymmetry, D, had to be estimated from the $I(003)/I(001)$ ratio, because of excess interference over the $d(005)$ peak. Interference over the other peaks could be removed by peak separation, using comparison between untreated and HCl-treated samples as guidance. As no information could be obtained about the oxidation state of Fe considerable uncertainty remains; the formula below is the one that fits the relationship found by Foster (Weaver 1989) between octahedral occupancy, number of trivalent octahedral cations and tetrahedral Al substitution:

$$(Si_{3.28}Al_{0.72})(Mg_{4.41},Fe^{2+}_{0.87},Fe^{3+}_{0.41}Al_{0.31})O_{10}(OH)_8 \quad [3]$$
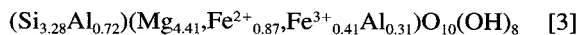
with $D = 0.79$, indicating significant concentration of Fe in the 2:1 layer. The formula is, of course, approximate only, due to the many assumptions involved.

The differential IR spectra of the rock samples are reported in Figures 2a and b; according to Farmer (1974), the positions of the OH-stretching bands, at 3574 and 3417 cm^{-1}, indicate an octahedral composition that is consistent with that estimated by XRD. The Si-O region, between 950 and 1100 cm^{-1}, is rather well-resolved; though the band position and intensity do not exactly match those reported for reference minerals, such high resolutions are observed only for minerals having low tetrahedral Al-for-Si substitution (van der Marel and Beutelspacher 1976). Furthermore, very little absorption was observed at both 820 and 760 cm^{-1}, the typical bands of tetrahedral Al-O vibrations:

this may be explained only by the combined effect of low tetrahedral Al and presence of Fe (Farmer 1974). It appears, then, that XRD and IR evidences are consistent in indicating low Al-for-Si substitution.

In the OH-bending region (600–700 cm^{-1}), a double feature appears at 650 and 694 cm^{-1}; the lowest frequency band was attributed to octahedral Mg and Fe. The highest frequency band is commonly attributed to octahedral Al (Farmer 1974: van der Marel and Beutelspacher 1976). This last interpretation is, however, in contrast with the number and position of the OH-stretching bands, which are quite different from those typical of high-Al chlorites (Farmer 1974; van der Marel and Beutelspacher 1976), with XRD results and also with the ease of dissolution in HCl, typical of trioctahedral chlorites. We can find no explanation for this; it is, however, to be noted that reference spectra for chlorites with low tetrahedral Al and containing significant amounts of Fe are, as far as we know, not available in literature.

XRD Diffraction of Soil Clay Fraction

The X-ray patterns of the BC horizon clay differ from those of the rock for the loss of thermal stability of the 1.4-nm peak, which shifted to about 1.2 nm when heated at 550 °C, indicating transformation of chlorite layers into vermiculite layers (Figure 3). Comparison of the integrated intensities of the 1.4- and 1.0-nm peaks indicated that chlorite and its weathering products are prevalent over illite in the soil clay fraction.
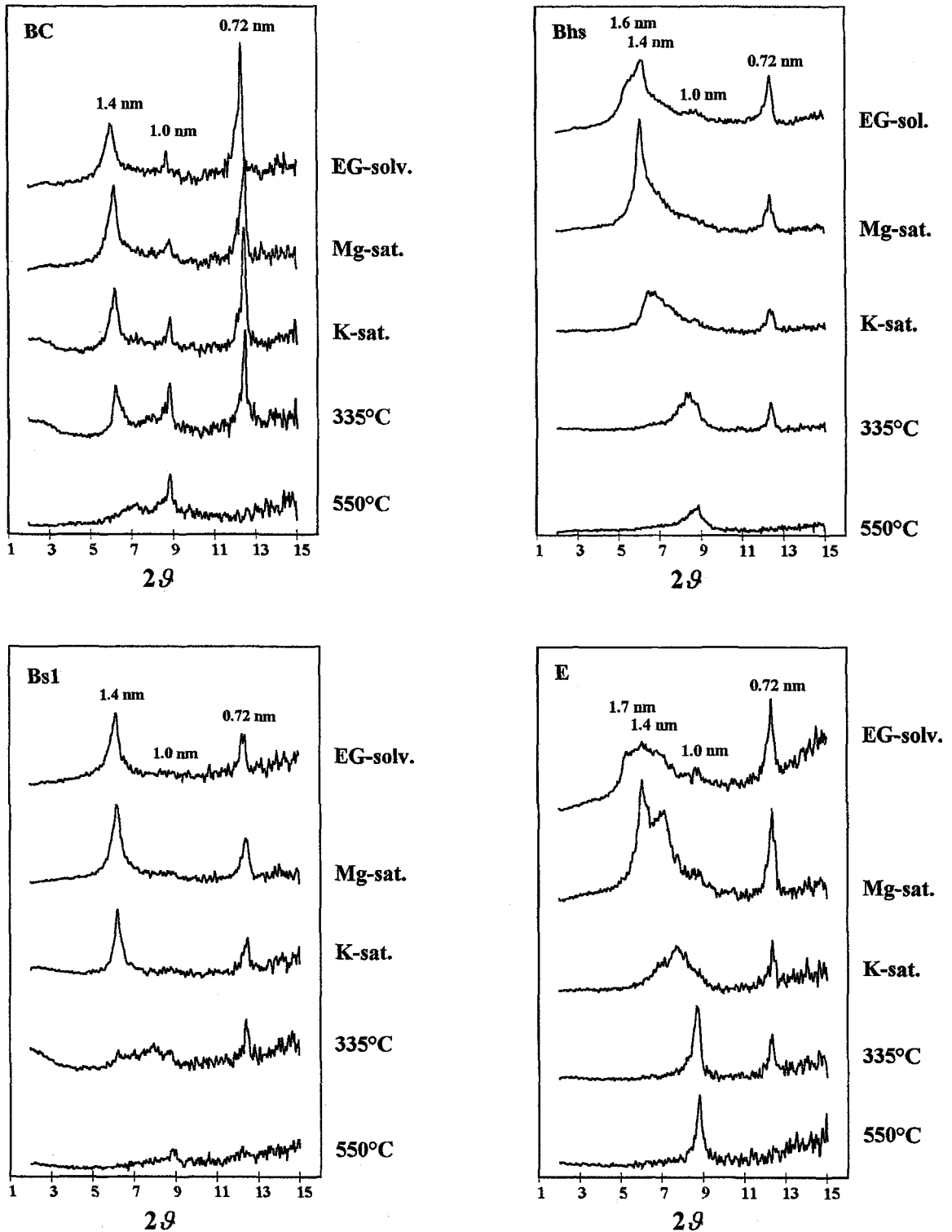
Figure 3.   X-ray patterns of soil clays (<2 μm) from 4 horizons, smoothed and corrected for Lorentz and polarization factors.

The treatment with Na-citrate produced much better-resolved patterns, where several interesting features appeared (Figure 4). A weak peak at about 3.1 nm, present in both Mg-saturated and EG-solvated slides, indicates some regular interstratification of chlorite and vermiculite. The 1.4-nm peak split into 2 components after EG-solvation (Figure 5): a minor one retaining the 1.43-nm spacing of parent chlorite, and a major one, at 1.52 nm, indicating presence of vermiculite layers. The ~0.7-nm peak, in the EG-solvated pattern, needed 3 basic components to be fitted. A broad one at 0.757 nm, integral with the 1.52 nm peak, was attributed to the $d(002)$ reflection of vermiculite; a small peak at 0.723 nm and a much more intense one at 0.712 nm could represent both chlorite $d(002)$ and kaolinite, though it was difficult to assign them to one or the other. K-saturation caused a marked reduction of intensity and a splitting of the 1.4-nm peak, with appearance of a broad reflection at ~1.1 nm; both features were absent in samples not treated with Na-citrate. Heating at 335 °C determined a further general shift of peaks towards 1.0 nm, while a 1.4-nm component was still apparent. At 550 °C, both an enhanced chlorite $d(001)$ reflection at 1.41 nm and a broad peak at 1.23 nm were visible, this last due to an interstratification between chlorite and an intermediate weathering product having partial vermiculite character but being more resistant to heating. Intensity of the 1.0-nm peak progressively increased with higher heating temperatures.

This combination of features indicates that, in the BC horizon, chlorite has partly transformed into 2 different hydroxy-interlayered vermiculitic components; in fact, only the interlayer of 1 component could be removed by Na-citrate. This different sensitivity might result from different compositions; for example, Righi et al. (1993) found that Mg-interlayers were scarcely sensitive to Na-citrate, while Al-interlayers are known to be removed in this way.

X-ray patterns of the clay fraction in the Bs2 horizon did not substantially differ from that of the underlying BC horizon, both before and after Na-citrate treatment, except for a reduction of intensity and a broadening of the illite peak at 1.0 nm, indicating that illite weathering was beginning at this level in the soil.

In the Bs1 horizon, the 1.0-nm peak is reduced at trace level; heating at 335 °C resulted in a more pronounced shift of the 1.4-nm peak towards 1.0 nm (Figure 3), evidencing less occupation of vermiculite interlayers by hydroxy polymers (Barnhisel and Bertsch 1989).

In the Na-citrate treated samples, the 3.1-nm peak was no longer observable; residual reflections still remained at 1.4 and 1.2 nm after heat treatments, but of much lower intensities (Figure 4). These changes seem to point to a progressive disappearance of the chlorite layers and of the regular chlorite-vermiculite interstratified mineral, a change frequently reported as a first stage in the weathering of chlorite (Senkayi et al. 1981: Herbillon and Makumbi 1975). Also, the equilibrium between the main components of the 0.7-nm peak had changed. The component at 0.71 nm had strongly decreased, consistently with previous observations indicating disappearing of chlorite; therefore, it is possible to identify the 0.72-nm component as kaolinite that increases relatively to chlorite (Figure 6).

Changes in mineralogy become more evident in the Bhs horizon (Figure 3). EG solvation caused the appearance of a shoulder on the low-angle side of the 1.4-nm peak, which could be resolved in a component with a d-spacing of 1.62 nm (Figure 7), a value consistent with a low-charge vermiculite (MacEwan and Wilson 1980; Douglas 1989). The 1.0-nm peak was extremely broad, and a new peak that was insensitive to EG solvation appeared at about 1.26 nm. This could indicate a random interstratified mica-vermiculite mineral. The sensitivity of the 1.4-nm multi-component peak to K-saturation and heating was much increased, though almost full shift to 1.0 nm was obtained only with heating at 335 °C, indicating a decreased, but still present, interlayer occupation.

Treatment with Na-citrate caused noticeable changes in X-ray traces (Figure 4). The EG-solvated sample was characterized by a main component with a d-spacing of 1.71 nm and by a minor one at 1.51 nm. The 1.0-nm peak decreased at trace level and the 1.2-nm component disappeared, the high-angle shoulder of the 1.5-nm peak in the Mg-saturated sample being actually resolved in a 1.4-nm component. The shift toward 1.0 nm after K-saturation was now much more evident, and collapse to 1.0 nm was complete after heating at 335 °C. The near absence of chloritic components at 1.4 nm in the 335 °C pattern, where the peak at 0.7 nm was still well evident, leads to attribute this peak mainly to kaolinite.

This series of characters suggests that the 2:1 minerals in this horizon include both smectitic and vermiculitic layers, with hydroxy-interlayers that hinder their expansion properties; interlayer polymers appear to be mainly aluminous, as evidenced by their easy removal by Na-citrate. The nature of the 1.2-nm mineral is unusual, in that its micaceous component seemed to have transformed to an expandable one after citrate treatment.

In the E horizon, the trends and characters visible in the Bhs become better expressed (Figure 3). Reactivity to EG was increased; the integral intensity of the lower-charge component is now greater with respect to the higher-charge one, and its d-spacing reaches 1.66 nm (Figure 8). The ~1.26-nm component was much more evident than in the Bhs, especially in the Mg-saturated condition, and appeared to expand slightly following EG-solvation, yielding a d-spacing of 1.28 nm as against 1.26 nm prior to solvation. The
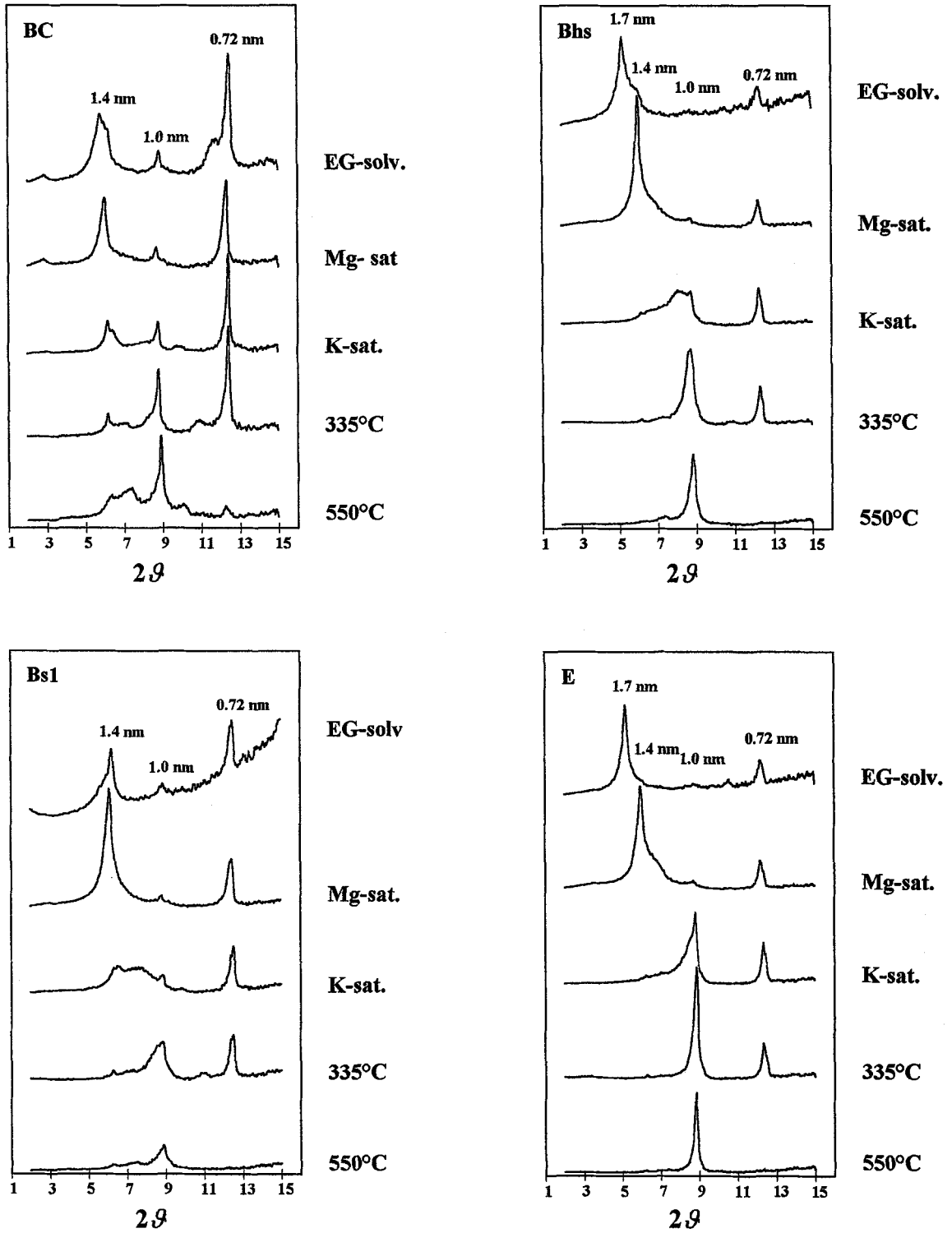
Figure 4.   X-ray patterns of soil clays ($<2 \ \mu$m) from 4 horizons, after Na-citrate treatment, smoothed and corrected for Lorentz and polarization factors.
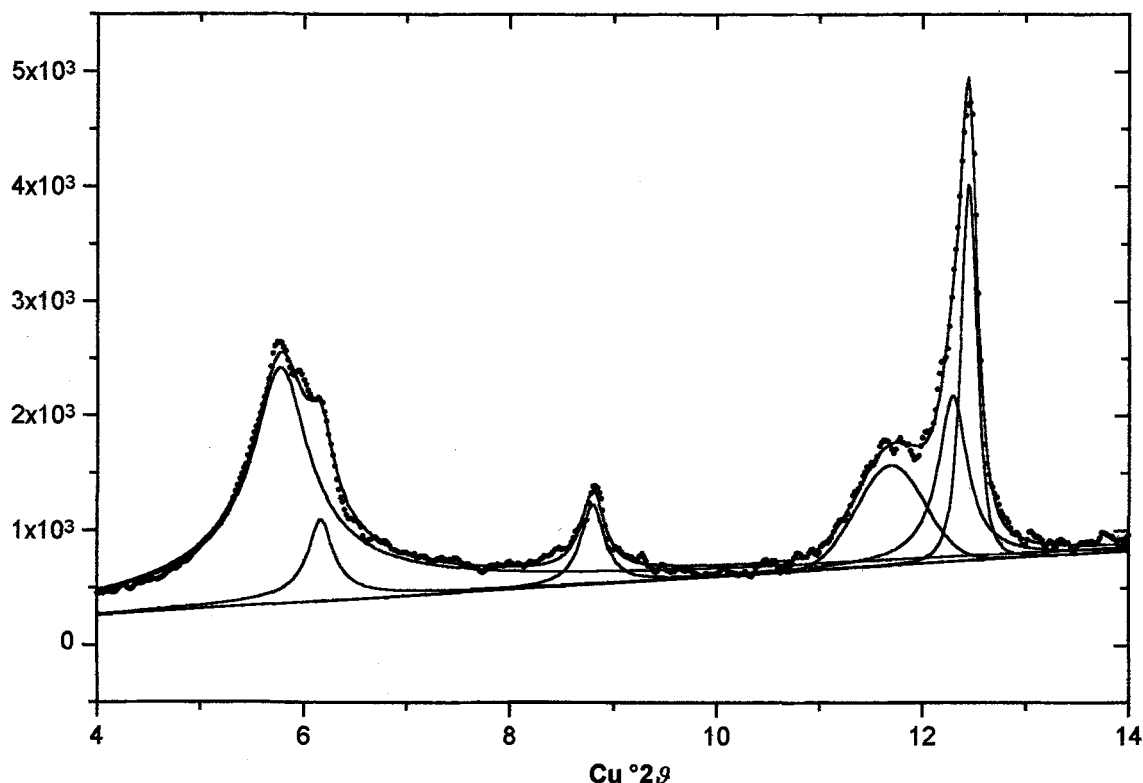
Figure 5. Peak separation of the X-ray pattern of soil clay, BC horizon, after Na-citrate treatment, EG-solvated. Full lines represent reconstructed peaks and fitted envelope curve; dots represent experimental data. Experimental traces previously corrected for Lorentz and polarization factors.

reaction to K-saturation and heating was more marked, as the effect produced in the Bhs by heating at 335 °C was here obtained at room temperature and a sharp 1.0-nm peak was obtained after heating.

The effect of Na-citrate treatment was similar, but more expressed, than in the Bhs (Figure 4); EG solvation yielded a single 1.71-nm peak, with only a very weak high-angle shoulder; the 1.26-nm component disappeared and full collapse to 1.0 nm was achieved by K-saturation. General characters of clay minerals in the E horizon thus appear similar to those of the Bhs horizon, the differences lying in a more smectitic nature of the 2:1 layers, in a larger amount of the unusual mica-vermiculite interlayered mineral and in a lower interlayer occupation by hydroxy-Al polymers.

Analysis of the $d(060)$ region in the various horizons showed how, in the BC horizon, both the 0.154-nm peaks from trioctahedral minerals and the 0.150-nm peaks from dioctahedral minerals were present, no semiquantitative estimate being possible because of the much higher relative intensity of mica's $d(060)$ peaks with respect to those of chlorite. Ascending in the profile (Figure 9), the 0.154-nm peak decreases progressively, being reduced to trace level in the Bhs and completely disappearing in the E. The gradual nature of this evolution points to a progressive

transformation from trioctahedral to dioctahedral structures, with increases in the contribution from expandable dioctahedral 2:1 minerals compensating for the fading out of illite.

IR Spectroscopy of Soil Clay Fraction

The IR spectra of the soil clay fractions showed a progressive evolution of the minerals from the BC horizon upwards, generally consistent with the XRD data.

In the OH-stretching region, it is possible to observe in the BC horizon the presence of an absorption band at about 3617 cm^{-1}, not present in the parent rock (Figure 2a); according to Farmer (1974), this band results from hydroxyl groups in the 2:1 octahedral sheet. In the Bs2 horizon, the 3620-cm^{-1} band increases in intensity, while the 3570-cm^{-1} component, due to the interlayer hydroxide sheet, shifts to about 3580 cm^{-1}, possibly due to a relative increase in the Mg contribution. In the Bs1, the major decrease in chlorite observed by XRD is further supported by the almost complete disappearance of the 3580-cm^{-1} band, while a peak at about 3695 cm^{-1} becomes visible; this last was attributed to kaolinite, after Farmer (1974). The only changes visible in the upper horizons are a de-
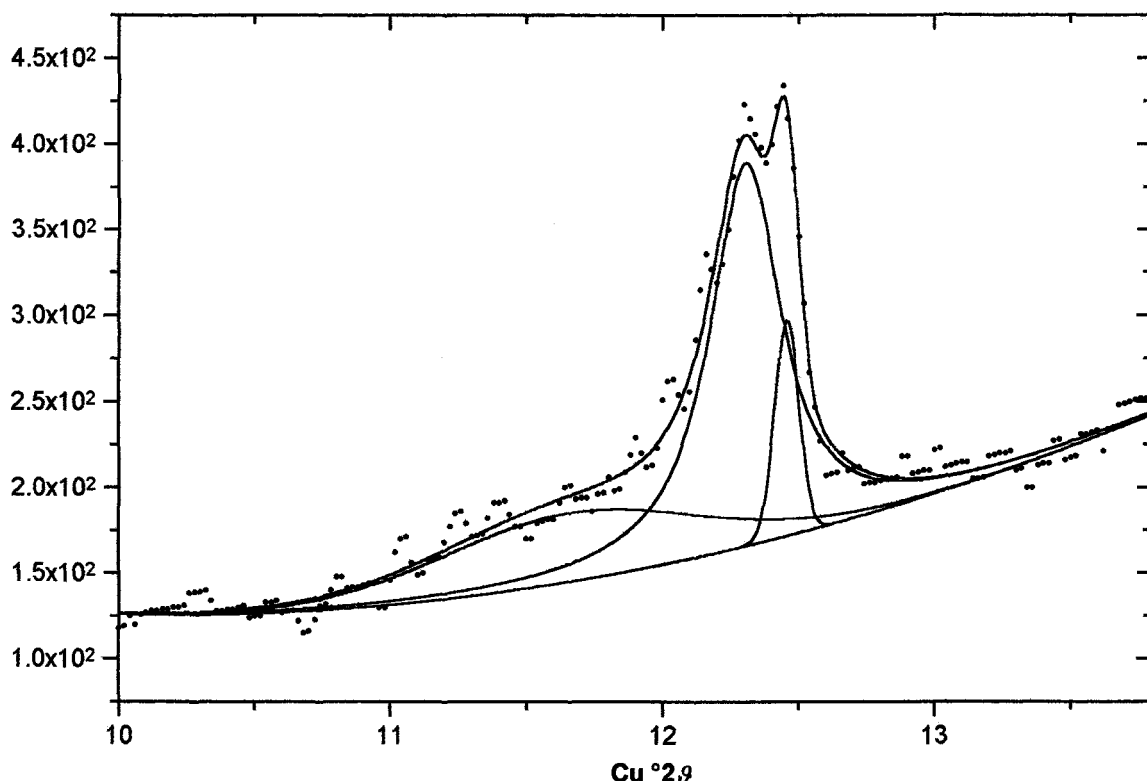
Figure 6. Peak separation of the X-ray pattern of soil clay, Bs1 horizon, after Na-citrate treatment and EG-solvation, in the 0.7-nm region. Same symbols as in Figure 5.

crease of the 3430-cm^{-1} band and, in the E horizon, an increased intensity of the kaolinite peak.

The modifications observable in the OH-deformation region are progressive towards the surface (Figure 2b); the OH-bending absorption from the chlorite hydroxide sheet, around 650 cm^{-1}, decreases, and disappears starting from the Bs1 horizon. Among the bands attributable to Al-OH deformations, the one at 915 cm^{-1} first appears in the BC horizon, and increases progressively towards the surface, together with the other one at 691 cm^{-1}, indicating growing proportions of dioctahedral layers. Few Al-O bands are observable, except for a weak one at about 765 cm^{-1}, in the upper horizons; on the other hand, the AlMgOH deformation band at 840 cm^{-1} that, according to Russell (1987), is typical of montmorillonite, is missing, so it is not possible to infer the nature of smectite from IR data.

In general, there is a striking resemblance between the IR spectra and those obtained by Senkayi et al. (1981) during a simulated laboratory weathering of a chlorite to smectite. The evolution of the spectra with time in Senkayi et al. (1981) is matched by the evolution observed here ascending from the rock to the E horizon. Also, the data of Proust et al. (1986), relative to a saprolite, are very similar to those obtained here for the lower horizons.

DISCUSSION

The results obtained by both XRD and IR characterization of the soil clays allow a progressive transformation sequence for parent rock chlorite to be outlined, consistent with other authors' results in both laboratory experiments and natural systems (Ross 1975: Ross and Kodama 1976: Herbillon and Makumbi 1975: Senkayi et al. 1981: Proust et al. 1986: Righi and Meunier 1991: Righi et al. 1993).

The first stage of chlorite weathering takes place in the oxidizing, acid and non-complexing environment of the lower solum. This stage involves Fe oxidation, partial removal of the original, Mg-rich hydroxide sheet and deposition of Al in the partially accessible interlayer space. These processes are typical of this kind of environment, as also pointed out by the experiments of Vicente et al. (1977) and Righi et al. (1990).

Some evidence that Fe is preferentially removed from the interlayer sheet is given by the shift to higher wavenumbers of the main interlayer OH-stretching band in the IR spectra from the Bs2 horizon, but this does not necessarily apply to the fate of Fe in the 2:1 layer. This Fe could be kept within the structure after oxidation (Senkayi et al. 1981; Proust et al. 1986), so contributing to layer charge reduction. The lower Fe
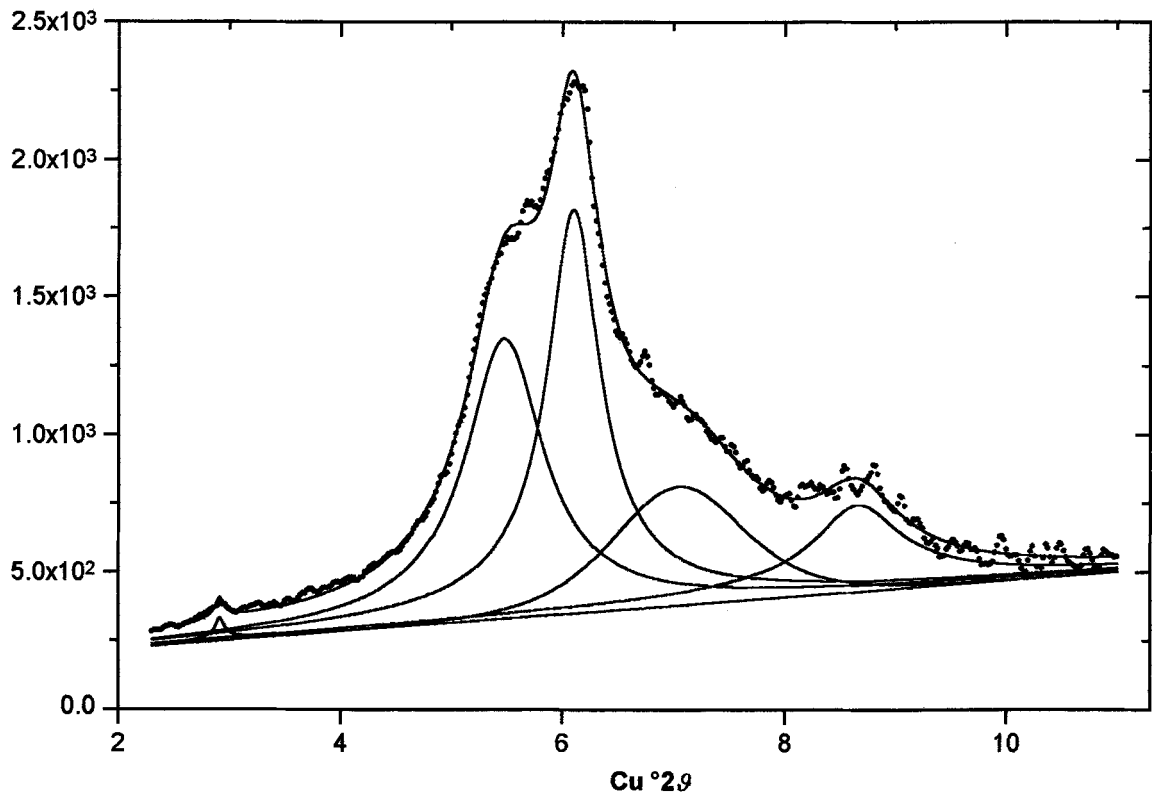
Figure 7. Peak separation of the X-ray pattern of soil clay, Bhs horizon, EG-solvated, 2.5 to 11 2θ region. Same symbols as in Figure 5.

content of the chlorite studied here, with respect to the one used by Senkayi et al. (1981), could lead to an initial weathering product having a relatively higher layer charge, as evidenced by failure to expand after Na-citrate treatment and EG solvation.

Another process known to take place in this weathering stage is the expulsion of Mg and, possibly, Fe, from the 2:1 octahedral sheet, where they may be replaced by Al. This process, together with Fe oxidation, causes a gradual change to a dioctahedral structure, stabilizing the mineral in the soil, and has been observed in both laboratory experiments (Ross 1975: Vicente et al. 1977: Senkayi et al. 1981) and natural systems (Proust et al. 1986). This hypothesis is supported in this soil by the progressive increase in intensity of the 3620-cm^{-1} and 915-cm^{-1} IR absorption bands and by the decrease of the 0.154-nm d(060) peak on going upwards in the profile.

The migration of Al from tetrahedral to octahedral positions, having lower free energy in aqueous environments, was observed by Vicente et al. (1977); besides substituting divalent cations in the 2:1 layer, the prevailing destination for this metal is the interlayer space. Our results showed that some Al accumulation in the interlayer takes place as soon as this space is made accessible by the partial removal of the (mainly

magnesian) hydroxide sheet of the parent chlorite; this was revealed by the possibility, already in the BC horizon, of removing part of the interlayers by the Na-citrate treatment. This Al migration would tend to further decrease layer charge; however, it is also likely that part of the Al found in the interlayers is coming from the soil solution or the exchange complex, where significant amounts of Al are present in this kind of soil.

In the soil surface horizons, the appearance of organic complexing agents modifies Al equilibria, favoring the solution phase; on the other hand, as the soil is subjected to significant erosion, surface horizons develop at the expense of the lower ones, and the modifications dictated by the different equilibria also involve minerals inherited from the lower solum. Consequently, Al interlayers in such minerals are removed, while the process of layer charge reduction continues, eventually bringing the 2:1 minerals to a smectitic nature. This sequence is observable in the X-ray patterns of the clay fraction of the soil, where, approaching the surface, 2:1 minerals become progressively more able to collapse to 1.0 nm after K-saturation and to expand to 1.7 nm following EG solvation. The presence of residual Al polymers in the interlayers of 2:1 minerals in surface horizons is evi-
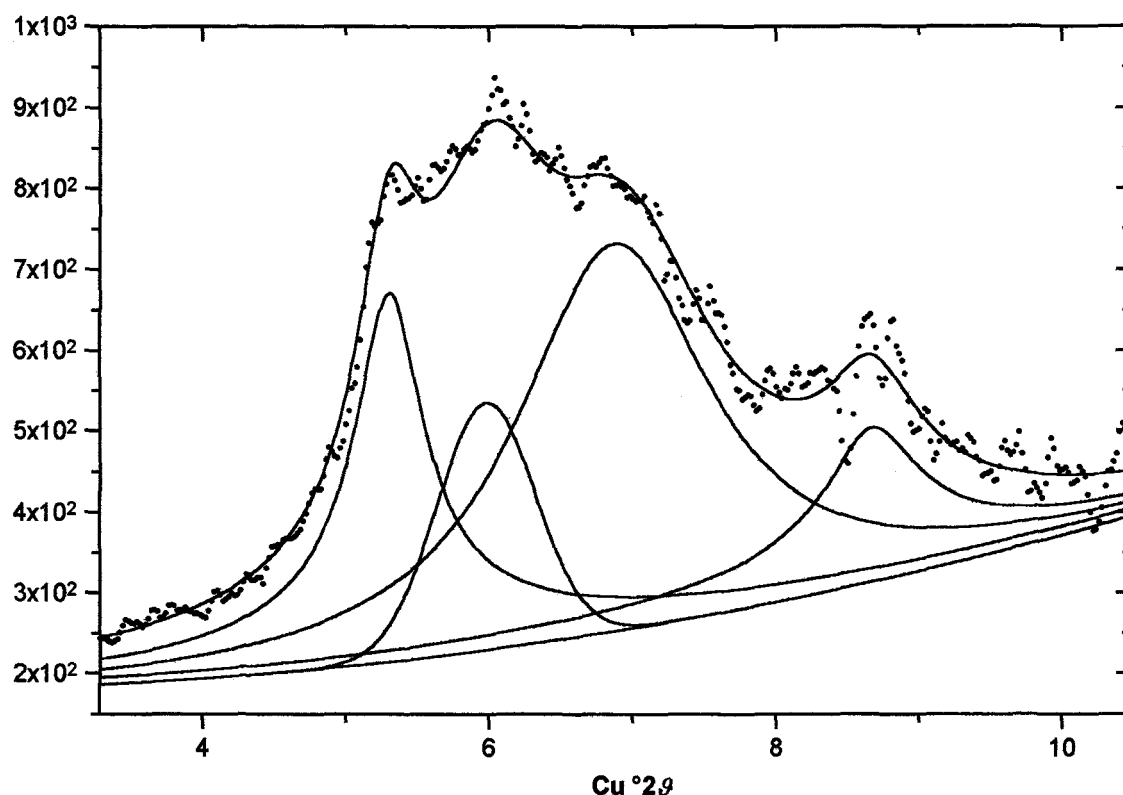
Figure 8. Peak separation of the X-ray pattern of soil clay, E horizon, EG-solvated, 2.5 to 11 2θ region. Same symbols as in Figure 5.

denced by the effects of Na-citrate treatment on X-ray patterns. This supports the hypothesis that these minerals originated in lower horizons, and are now modified as a result of profile lowering by erosion, rather than having formed directly from the weathering of primary minerals in an upper horizon environment.

The contribution of illite and its weathering products to this sequence is not very clear. Illite is a secondary component of the clay fraction, and its transformation probably follows a pathway similar to that of chlorite. Illite appears to start weathering higher up in the profile than chlorite, where the bulk of the 2:1 expandable component is already present, and it is probably contributing to the formation of the higher-charged expandable components observed in the Bhs horizon.

When considering the origin of the low-charge expandable mineral in the surface horizons, some alternative hypotheses have to be considered. The airborne dust hypothesis of Coen and Arnold (1972) does not

fit with these soils, as 2 basic points of their reasoning, low clay content and scarcity of phyllosilicates in lower solum and parent rock, are clearly absent. It is instead not possible to rule out completely the hypothesis that Al-interlayers never formed, or formed badly, in the upper horizons, where the low-charge mineral would then have formed directly from chlorite weathering. This would be consistent with the kind of differentiation in chemical environments typical of podzolization; however, our interpretation concerning the evolution of the soil profile studied leads us to consider this hypothesis less probable.

The random mica-vermiculite interlayered mineral, observed mainly in the E horizon and, to a lesser extent, in the Bhs, deserves some special consideration. It is unlikely that this mineral represents an intermediate stage in the vermiculitization of illite, as its appearance, in the Bhs, does not coincide with the main decrease of illite content taking place in the Bs1. This interlayered mineral is mostly represented in the E ho-

→

Figure 9. Evolution of the region containing $d(060)$ peaks of clay minerals: a) BC horizon, b) Bs2 horizon, c) Bs1 horizon, d) Bhs horizon, e) E horizon. The first peak on the left side is due to quartz; the second peak from the left in a) through d) is the ~1.54-nm $d(060)$ of trioctahedral structures, decreasing progressively and missing in e). The rightmost peak, increasing from a) to e), is the 1.50-nm $d(060)$ peak of dioctahedral structures.
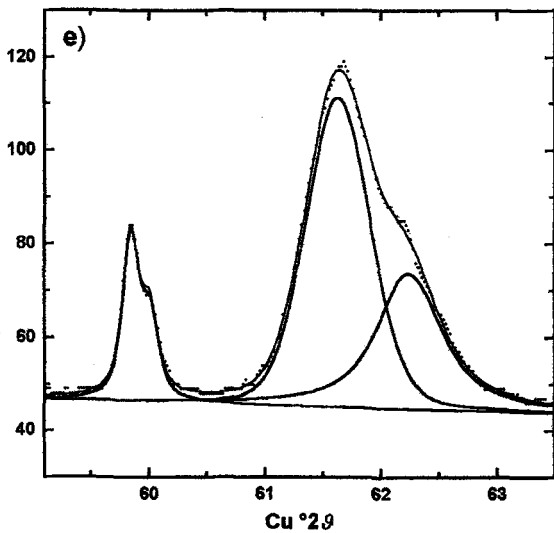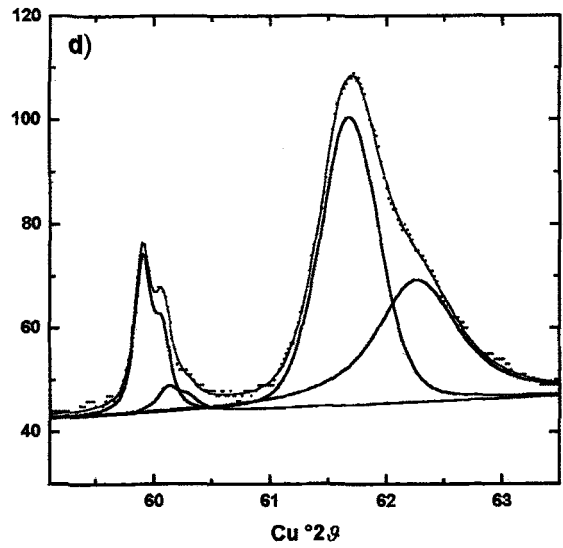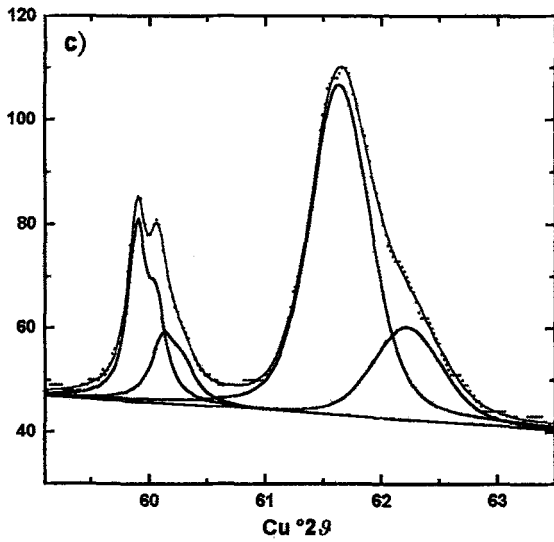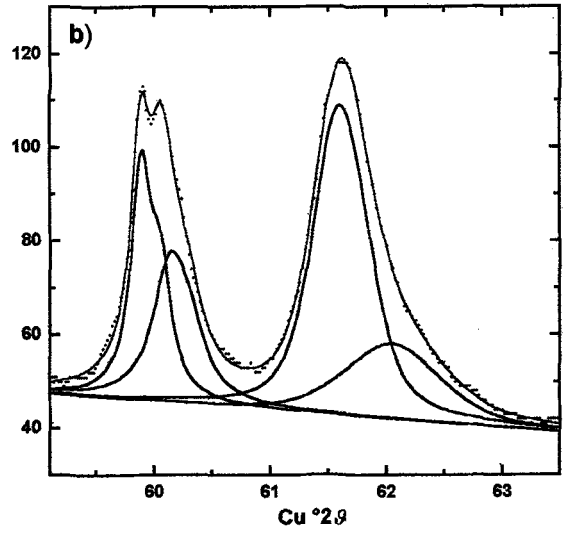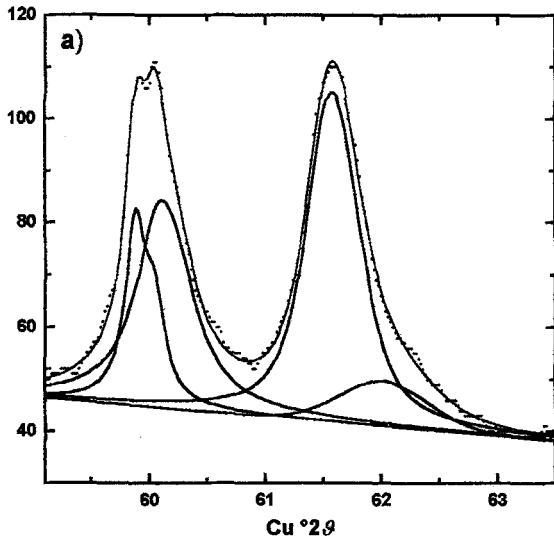
rizon, suggesting that its formation takes place mainly at the soil surface; an unusual feature of this mineral is the apparent loss of illite characters after Na-citrate treatment.

Soil solution data (Carnicelli et al. 1994), relative to a nearby similar profile, have shown a sudden disappearance of K in the passage from the surface to the underneath horizons. These observations indicate that the illite-vermiculite interlayered mineral may result from partial K fixation by the higher-charged expanding components. Potassium, held less strongly than in true illites, could then be removed in the Na-citrate treatment, by enhanced exchange with Na due to the high temperatures and pressures of the treatment. The K-fixation process, promoted by wetting-drying cycles, was observed by Eberl et al. (1986), while Ross (1980) noted the generally high K selectivity of the clays in Spodosol surface horizons; frequent wetting and drying cycles actually take place in the surface horizons of the soil studied, in the warm spring-summer period.

Kaolinite is present in small amounts in the parent rock; interference from various $d(002)$ reflections hampered semiquantitative estimates of its content in the clay fraction along the profile. A slight increase towards the surface cannot be excluded, but it is nevertheless of minor importance.

CONCLUSIONS

The results of this investigation on a natural system substantially support the hypothesis of Ross (1980) regarding the possibility of transformation of trioctahedral ferruginous chlorite into dioctahedral smectite in Spodosols.

Up until now, this kind of transformation has been observed without ambiguity only in laboratory experiments or in different kinds of soil; the results obtained here have evidenced it in a less ambiguous manner, by observation of a weathering sequence in which interference from mica minerals is reduced, thanks to their limited presence in the clay fraction.

ACKNOWLEDGMENTS

REFERENCES

April RH, Hluchy MM, Newton RM. 1986. The nature of vermiculite in Adirondack soils and till. Clays Clay Miner 34:549–556.

Bailey SW. 1975. Chlorites. In: Gieseking JE, editor. Soil components, vol 2: Inorganic components. Berlin: Springer-Verlag. p 191–263.

Barnhisel RI, Bertsch PM. 1989. Chlorites and hydroxy-interlayered vermiculite and smectite. In: Dixon JB, Weed SB, editors. Minerals in soil environments. Madison, WI: Soil Sci Soc Am. p 729–788.

Brown G, Brindley GW. 1980. X-ray diffraction procedures for clay mineral identification. In: Brindley GW, Brown G,

editors. Crystal structures of clay minerals and their X-ray identification. London: Mineral Soc. p 305–360.

Carnicelli S, Cecchini G, Mirabella A, Sanesi G. 1994. Composizione della soluzione e mineralogia della frazione argillosa nei suoli delle faggete di Pian di Novello (PT). Atti del XII Congresso della Società Italiana di Chimica Agraria; 1994; Piacenza. p 57–64.

Cho HD, Mermut AR. 1992. Evidence for halloysite formation from weathering of ferruginous chlorite. Clays Clay Miner 40:608–619.

Coen GM, Arnold RW. 1972. Clay mineral genesis of some New York Spodosols. Soil Sci Soc Am Proc 36:342–350.

Dallan L, Puccinelli A, Verani M. 1981. Geologia dell'Appennino Settentrionale tra l'alta Val di Lima e Pistoia (note illustrative della carta geologica alla scala 1:25,000). Boll Soc Geol It 100:567–586.

Douglas LA. 1989. Vermiculites. In: Dixon JB, Weed SB, editors. Minerals in soil environments. Madison, WI: Soil Sci Soc Am. p 635–674.

Eberl DD, Środoń J, Northrop HR. 1986. Potassium fixation by wetting and drying. In: Davis JA, Hayes KF, editors. Geochemical processes at mineral surfaces. Am Chem Soc Symp Ser 323:296–326.

Enzo S, Fagherazzi G, Benedetti A, Polizzi S. 1988. A profile-fitting procedure for analysis of broadened X-ray diffraction peaks: I. Methodology. J Appl Crystallogr 21:536–542.

Farmer VC. 1974. The layer silicates. In: Farmer VC, editor. The infrared spectra of minerals. Monograph 4. London: Mineral Soc. p 331–363.

Herbillon AJ, Makumbi MN. 1975. Weathering of chlorite in a soil derived from a chloritoschist under humid tropical conditions. Geoderma 13:89–104.

Howard SA, Preston KD. 1989. Profile fitting of powder diffraction patterns. In: Bish DL, Post JE, editors. Modern powder diffraction. Reviews in mineralogy, 20. Washington DC: Mineral Soc Am. p 217–275.

MacEwan DMC, Wilson MJ. 1980. Interlayer and intercalation complexes of clay minerals. In: Brindley GW, Brown G, editors. Crystal structures of clay minerals and their X-ray identification. London: Mineral Soc. p 197–248.

Malcolm RL, Nettleton WD, McCracken RJ. 1969. Pedogenic formation of montmorillonite from a 2:1–2:2 intergrade clay mineral. Clays Clay Miner 16:405–414.

Marel HW van der, Beutelspacher H. 1976. Atlas of infrared spectroscopy of clay minerals and their admixtures. Amsterdam: Elsevier Science. 396 p.

Moore DM, Reynolds RC Jr. 1989. X-ray diffraction and the identification and analysis of clay minerals. Oxford: Oxford Univ Pr. 332 p.

Proust D, Eymery JP, Beaufort D. 1986. Supergene vermiculitization of a magnesian chlorite: Iron and magnesium removal processes. Clays Clay Miner 34:572–580.

Righi D, Bravard S, Chauvel A, Ranger J, Robert M. 1990. In situ study of soil processes in an Oxisol-Spodosol sequence of Amazonia (Brazil). Soil Sci 150:438–445.

Righi D, Meunier A. 1991. Characterization and genetic interpretation of clays in an acid brown soil (Dystrochrept) developed in a granitic saprolite. Clays Clay Miner 39:519–530.

Righi D, Petit S, Bouchet A. 1993. Characterization of hydroxy-interlayered vermiculite and illite/smectite interstratified minerals from the weathering of chlorite in a Cryorthod. Clays Clay Miner 41:484–495.

Ross GJ. 1975. Experimental alteration of chlorites into vermiculites by chemical oxidation. Nature 255:133–134.

Ross GJ. 1980. The mineralogy of Spodosols. In: Theng BKG, editor. Soils with variable charge. Lower Hutt, New

Zealand: Soil Bureau, Department of Scientific and Industrial Research. p 127–143.

Ross GJ, Kodama H. 1976. Experimental alteration of a chlorite into a regularly interstratified chlorite-vermiculite by chemical oxidation. Clays Clay Miner 24:183–190.

Russell JD. 1987. Infrared methods. In: Wilson MJ, editor. A handbook of determinative methods in clay mineralogy. Glasgow: Blackie. p 133–173.

Senkayi AL, Dixon JB, Hossner LR. 1981. Transformation of chlorite to smectite through regularly interstratified intermediates. Soil Sci Soc Am J 45:650–656.

Tamura T. 1958. Identification of clay minerals from acid soils. J Soil Sci 9:141–147.

Vicente MA, Razzaghe M, Robert M. 1977. Formation of aluminium hydroxy vermiculite (intergrade) and smectite from mica under acidic conditions. Clay Miner 12:101–111.

Wada K, Kakuto Y, Wilson MA, Hanna JV. 1991. The chemical composition and structure of a 14 Å intergradient mineral in a Korean Ultisol. Clay Miner 26:449–461.

Weaver CE. 1989. Clays, muds and shales. Developments in sedimentology, 44. Amsterdam: Elsevier Science. 819 p.

Wilson MJ. 1986. Mineral weathering processes in Podzolic soils on granitic materials and their implications for surface water acidification. J Geol Soc, London 143:691–697.

Wilson MJ. 1987. X-ray powder diffraction methods. In: Wilson MJ, editor. A handbook of determinative methods in clay mineralogy. Glasgow and London: Blackie. p 26–98.